Advanced and Sustainable Technologies
ASET
E-ISSN 2976-2294
Volume 5, No 1, June 2026 [244-261]

IoT-Driven Vibration Sensing and Decision-Tree Analytics for Multi-Class Tyre Pressure Diagnostics

Mohd Saifunnaim bin Mat Zain[1]* and Ahmad Kadri bin Junoh[2]

[1]Advanced Technology College Jitra Campus, Department of Manpower, Ministry of Human Resource, Bandar Darulaman, 06000 Jitra, Kedah, Malaysia.
[2]Faculty of Intelligent Computing, Universiti Malaysia Perlis (UniMAP), 02600 Arau, Perlis, Malaysia.

Received 31 December 2025, Revised 27 February 2026, Accepted 15 March 2026

ABSTRACT

Maintaining correct tire pressure is essential for ensuring vehicle safety, fuel efficiency, and ride stability. However, conventional tire pressure monitoring systems commonly rely on direct pressure sensors or indirect wheel-speed estimation, which limits diagnostic resolution and scalability for multi-level pressure conditions. This study introduces an IoT-enabled vibration-based monitoring framework that leverages machine learning for improved accuracy and interpretability to assessing tire pressure states. Four MPU-9250 triaxial accelerometers were mounted near each tire and interfaced with a Raspberry Pi 5 using a TCA9548A I^2C multiplexer. Vibration signals were collected at nine distinct tire pressure levels, ranging from optimal to progressively lower pressure. Time-domain features and frequency-domain characteristics were extracted to capture tire–road interaction dynamics influenced by pressure changes. A decision tree classifier was employed to evaluate the separability and diagnostic performance across all classes. The model achieved clear discrimination between optimal and low-pressure states, confirming that vibration signatures contain sufficient information for reliable, multi-class pressure detection. The system integrates a MariaDB backend, a Flask-based dashboard, and secure remote connectivity to enable real-time monitoring. The results demonstrate that IoT-driven vibration sensing, combined with interpretable machine-learning analytics, offers a low-cost, scalable, and accurate alternative to conventional TPMS for intelligent, adaptive vehicle maintenance.

Keywords: IoT, Vibration sensing, Tyre pressure diagnostics, Signal processing, Decision tree.

1. INTRODUCTION

Maintaining correct tyre pressure is essential for vehicle safety, fuel efficiency and tyre longevity. Deviations from optimal pressure alter tyre stiffness, contact patch dynamics, and vibration transmission through the suspension and vehicle structure, ultimately degrading handling stability and increasing accident risk. While conventional tyre pressure monitoring systems rely on direct pressure sensors or indirect wheel-speed estimation, these approaches often provide limited diagnostic resolution and are constrained in scalability when multiple pressure levels or distributed monitoring are required.

Vibration-based tyre pressure diagnostics present an attractive alternative because pressure variations directly influence tyre–road interaction dynamics and the resulting structural vibration signatures [1]. However, this approach is technically challenging. Tyre-induced vibration signals are low in amplitude, strongly affected by road conditions, vehicle speed,

*Corresponding author: m.saifunnaim@jtm.gov.my

suspension dynamics, and environmental noise, and often overlap across pressure states, resulting in low signal-to-noise ratios and subtle inter-class differences that complicate reliable multi-class discrimination under real driving conditions [2].

Existing research has demonstrated that vibration signals can be used for condition monitoring and fault diagnosis in mechanical and automotive systems. Prior studies have explored time-domain, frequency-domain, and time–frequency features combined with machine learning models such as support vector machines, neural networks, and deep learning architectures. While promising results have been reported, most studies focus on binary or limited-class classification problems and are frequently evaluated under controlled laboratory conditions, limiting their applicability to real-world multi-class tyre pressure diagnostics [3].

The primary objective of this study is to develop and validate an IoT-driven vibration-based diagnostic framework capable of reliably identifying multiple tyre pressure states under real driving conditions, using interpretable, computationally efficient machine-learning analytics. To achieve this objective, the proposed system integrates multiple low-cost triaxial accelerometers with an edge-computing platform to enable synchronized, real-time vibration acquisition from all four tyre locations. Instead of relying on complex black-box models, a decision-tree classifier is adopted due to its interpretability, low computational overhead, and suitability for embedded automotive deployment [4].

The proposed framework is experimentally validated using real driving data collected across nine distinct tyre pressure classes, ranging from ideal to progressively under-inflated conditions. The results demonstrate that vibration signatures contain sufficient discriminatory information for accurate multi-class pressure diagnosis while maintaining practical deployability within an IoT-enabled vehicle monitoring architecture [5].

The remainder of this paper is organized as follows: Section II describes the proposed IoT-based system architecture and experimental methodology; Section III presents the results of vibration signal analysis and decision-tree classification; and Section IV concludes with key findings and future research directions.

2. METHODOLOGY

The research employs a mixed-methods design, integrating experimental IoT-based vibration data acquisition with computational decision-tree modelling. Following the approach of [6], vibration signals from tyre pressure systems are collected in situ using a sensor network. The design combines empirical signal measurements with advanced signal processing and machine learning techniques to accurately classify multi-class tyre pressure conditions. [7] emphasizes optimizing sample size, data points, and augmentation in vibration analysis, which underpins the experimental design and ensures sufficient, robust data for model training and validation.

The theoretical framework bridges IoT-enabled sensor network data streams with computational vibration signal analysis and interpretable decision-tree models, as proposed by [8,9]. This framework conceptualizes vibration signals as multiscale time-frequency data features indicative of varying tyre pressure states. Sampling comprises tyres under diverse operational conditions encompassing multiple types and inflation pressures encountered in automotive applications. Sampling strategies, inspired by [10,11], use stratified sampling to reflect tire heterogeneity and operating scenarios, thereby improving model generalizability. Data collected includes real-time vibration readings from numerous tyre samples, ensuring representative and variable pressure states for model training.

2.1 Sensor Deployment

Vibration sensors are pivotal components in IoT-based tyre pressure diagnostics systems, tasked with capturing mechanical vibration signals that are indicative of tyre health and pressure conditions. According to [12,13], accelerometers and piezoelectric sensors are widely used in IoT environments for vibration detection. Accelerometers offer multi-axis sensitivity and high precision, making them suitable for capturing dynamic tyre vibrations during vehicle operation. On the other hand, Piezoelectric sensors convert mechanical strain directly into electrical signals, enabling robust and noise-resistant measurements in harsh environments like vehicular systems.

Sensors include piezoelectric accelerometers and microelectromechanical systems (MEMS) vibration sensors, integrated with microcontrollers and wireless communication modules. A 9-axis unit, such as the MPU-9250, shown in Figure 1, integrates a three-axis MEMS gyroscope, a three-axis MEMS accelerometer, and a three-axis magnetometer, following designs from [14,15]. The sensor nodes are designed for low-power operation and real-time data acquisition in vehicular environments, with wireless transmission enabled via integrated microcontrollers and communication modules. While the MPU-9250 provides adequate bandwidth and sensitivity for general motion and vibration monitoring, capturing subtle vibration variations caused to tyre pressure changes may require complementary high-sensitivity accelerometers or advanced signal-processing techniques.

Figure 1: MPU-9250 nine-axis inertial measurement unit integrating a three-axis gyroscope, accelerometer, and magnetometer.

Strategically deploying the sensor directly on tyres or the vehicular suspension enables comprehensive monitoring of the vibration signatures associated with various tyre pressure states. Sensor placement on tyres typically targets the inner liner, tread, or sidewall areas, where deformation and dynamic forces are most pronounced during pressure variation. Placement on the chassis or suspension arms complements tyre sensors by capturing transmitted vibration signatures, facilitating a holistic understanding of vehicle-road interactions. Design considerations must include sensor size, weight, power requirements, and environmental resilience to optimize long-term reliability inside the complex dynamics of tyre movements and road contact. The combination of sensor types and locations enhances fault-detection reliability by leveraging diverse vibration-signal sources.

Accurate placement of vibration sensors is a critical factor in ensuring reliable acquisition of structural vibration signatures related to tire–road interaction. In this study, multiple MPU-9250 inertial measurement units (IMUs) were installed at strategic locations within the cabin of a Honda Jazz GK to capture vibration responses under different tire pressure conditions. The sensor placement strategy was designed to balance mechanical coupling to the vehicle structure, signal sensitivity, wiring practicality, and real-world automotive constraints. The experimental platform is a Honda Jazz GK passenger vehicle operated under real driving conditions. Sensor installation was conducted entirely within the vehicle cabin, avoiding direct exposure to harsh external environments such as water, debris, and excessive thermal variation. This approach

enhances system durability while still allowing effective transmission of vibration energy from the tire–road interface through the vehicle chassis.

The MPU-9250 sensors were mounted on rigid metallic body panels near the wheel wells using adhesive tape and secured wiring, as shown in Figure 2. These locations provide direct mechanical coupling to structural elements influenced by wheel-induced vibrations. Four MPU-9250 sensors were deployed to correspond with the four tire locations:

a) Sensor 1 (Front Left – FL): Mounted near the front-left wheel well on the interior body panel. This position captures vibration signals generated by steering input, road irregularities, and braking forces acting on the front-left tire.
b) Sensor 2 (Front Right – FR): Installed symmetrically opposite Sensor 1 on the front-right side. This configuration enables comparative analysis of left- and right-front tire dynamics and improves robustness against localized structural resonance.
c) Sensor 3 (Rear Left – RL): Positioned near the rear-left wheel well inside the luggage compartment area. The sensor is mechanically coupled to the rear chassis structure, capturing vibration signatures influenced by load distribution and rear suspension behavior.
d) Sensor 4 (Rear Right – RR): Mounted at a corresponding location on the rear-right side. Together with Sensor 3, this allows analysis of rear axle vibration asymmetry and improves classification reliability across different tire pressure classes.

This symmetric sensor placement, illustrated in Figure 3, ensures spatial coverage across the entire vehicle footprint and enables correlation of vibration features with specific tire positions. The selected sensor locations are particularly suitable for tire pressure monitoring based on vibration signatures, as underinflated tires are known to induce increased vibration amplitude and variability due to changes in tire stiffness and contact patch dynamics. Vibrations generated at the tire–road interface propagate through the suspension system and vehicle chassis, making the chosen cabin-mounted locations effective for indirect pressure estimation.

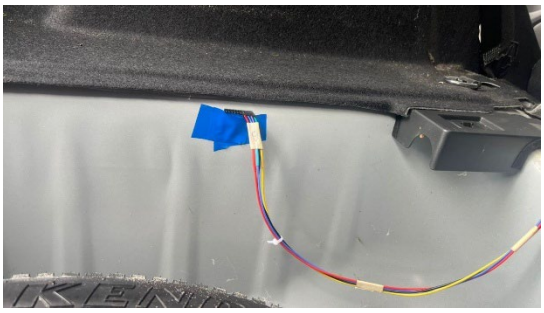

Figure 2: MPU-9250 sensors were mounted on body panels near the wheel wells using adhesive tape and secured wiring.

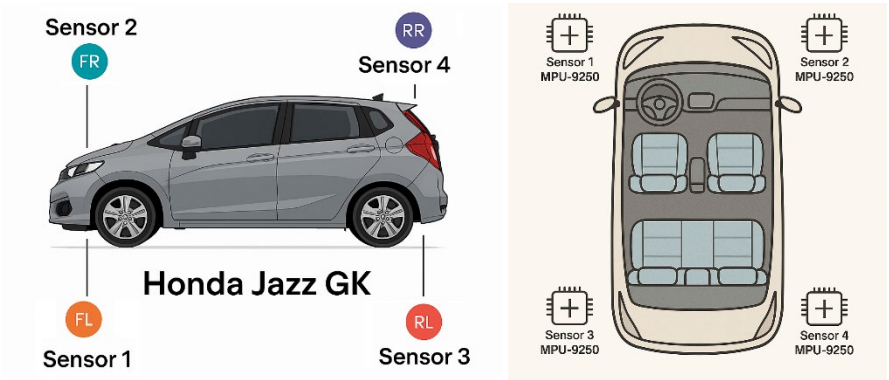

Figure 3: MPU-9250 sensors location and position in the Honda Jazz GK passenger vehicle.

2.2 Hardware and Software Components

The proposed IoT-based vibration monitoring system integrates hardware and software components (Table 1) to ensure reliable data acquisition, processing, storage, visualization, and remote accessibility. The MPU-9250 inertial measurement unit serves as the primary sensing element, functioning as a triaxial accelerometer to capture vibration signals along the X, Y, and Z axes. These vibration signatures are critical for characterizing tyre condition and vehicle dynamic behavior. To accommodate multiple MPU-9250 sensors sharing the same I^2C address, a TCA9548A I^2C multiplexer is employed. This component expands the I^2C communication capability of the system by enabling channel-based sensor selection, thereby preventing address conflicts and ensuring synchronized data acquisition.

At the core of the system, the Raspberry Pi 5 operates as the central processing and control unit. It manages sensor communication, executes data acquisition scripts, and hosts local services for storage and visualization. Acquired vibration data are stored in a MariaDB relational database, which efficiently handles time-stamped sensor measurements and supports structured querying for subsequent analysis. MySQL Workbench is utilized as a graphical database management interface, enabling efficient inspection, debugging, and validation of stored datasets during system development and experimentation.

From a software perspective, Python is adopted as the primary programming language due to its extensive library support and compatibility with embedded platforms. Python scripts handle sensor initialization, real-time data parsing, database communication, and system-level integration. A lightweight Flask web framework is deployed on the Raspberry Pi to provide a web-based interface and application programming interface (API) for real-time data access and visualization. For front-end visualization, the web dashboard integrates Chart.js, a JavaScript-based plotting library, to display live vibration waveforms and system status intuitively. To enable secure remote monitoring and system management, Tailscale is implemented as a virtual private network (VPN), allowing encrypted peer-to-peer access to the Raspberry Pi from external networks without exposing public IP addresses. Additionally, RealVNC Viewer is employed to provide remote graphical desktop access, facilitating system configuration, troubleshooting, and maintenance. Collectively, these hardware and software components form a cohesive and scalable platform suitable for real-world automotive vibration monitoring and intelligent tyre condition assessment applications.

Table 1: List of hardware and software components.

Component	Type	Function / Description
MPU-9250	Sensor	Triaxial accelerometer for capturing vibration data
TCA9548A	I2C Multiplexer	Expands I2C communication channels to handle multiple sensors
Raspberry Pi 5	Microcontroller	Central processing and data management unit
MariaDB	Database	Stores time-stamped vibration data for query and analysis
MySQL Workbench	Database GUI	Used for visualizing and managing the MariaDB database
Python	Programming Language	Used for data parsing, acquisition, and communication
Flask	Web Framework	Provides web interface and real-time visualization API
Chart.js	JavaScript Library	Plots real-time sensor data in the web dashboard
Tailscale	VPN	Enables secure remote access to the Raspberry Pi
RealVNC Viewer	Remote Desktop Tool	Provides GUI access to the Raspberry Pi interface

2.3 Hardware and Software Configuration

The hardware architecture of the proposed system is designed to ensure reliable, continuous data acquisition, processing, and remote accessibility, as illustrated in Figure 4. The system integrates four MPU-9250 inertial measurement units (IMUs), each functioning as a tri-axial accelerometer, interfaced through a TCA9548A I^2C multiplexer and centrally managed by a Raspberry Pi 5. The MPU-9250 is widely adopted in vibration and motion-sensing applications due to its high sensitivity, compact size, and suitability for embedded systems [16].

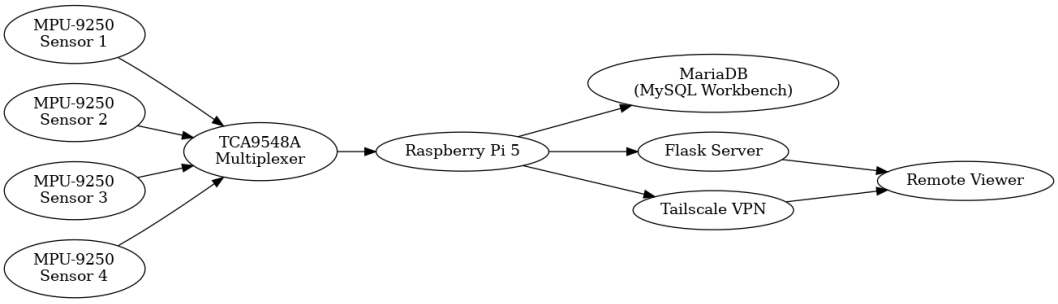

Figure 4: The overall system architecture, showing the connection between four MPU-9250 accelerometers, the TCA9548A I2C multiplexer, the Raspberry Pi 5, the MariaDB database, Flask server, and the remote monitoring client connected through Tailscale VPN.

Each MPU-9250 sensor acquires vibration signals along the X, Y, and Z axes, enabling comprehensive capture of dynamic responses associated with tire–road interactions. Since all MPU-9250 devices share the same I^2C address, the TCA9548A multiplexer is used to enable sequential sensor communication by dynamically selecting individual I^2C channels. This strategy effectively eliminates address conflicts while ensuring synchronized, scalable data acquisition across multiple sensing nodes. The Raspberry Pi 5 operates as both the central controller and edge-computing platform, responsible for sensor polling, data preprocessing, and local data management. All acquired vibration data are systematically stored in a MariaDB database, allowing structured storage and efficient retrieval for further analysis. A Flask-based web server is deployed on the Raspberry Pi to provide a lightweight, responsive, real-time visualization interface, a feature commonly adopted in IoT-based monitoring systems [17].

A Tailscale virtual private network (VPN) is configured to provide secure global access, enabling encrypted remote monitoring and system management without exposing devices to public networks. This approach enhances cybersecurity and reliability, which are critical requirements in connected automotive and industrial IoT deployments [18]. The Raspberry Pi 5 communicates with the sensing layer via the I^2C protocol using the standard SDA and SCL lines, which interface directly with the TCA9548A I^2C multiplexer. Each of the four MPU-9250 inertial measurement units (IMUs) is connected to a dedicated output channel of the multiplexer (CH0–CH3). As all MPU-9250 sensors share the same default I^2C address (0x68), address conflicts are resolved by the multiplexer's channel-switching mechanism, which enables sequential, isolated access to each sensor. The resulting I^2C communication topology, illustrated in Figure 5, depicts the routing of individual MPU-9250 devices through the TCA9548A to the Raspberry Pi's GPIO interface. This structured, scalable communication framework ensures robust, reliable data transmission while enabling straightforward system expansion, making it well-suited for real-world automotive vibration monitoring and tire-condition sensing applications.

The GPIO wiring configuration of the proposed system is designed to support reliable multi-sensor communication while maintaining simplicity and scalability. The Raspberry Pi 5 interfaces with the TCA9548A I^2C multiplexer via the standard I^2C communication protocol using the Serial Data (SDA) and Serial Clock (SCL) lines available on the Raspberry Pi's GPIO header. These lines

serve as the primary communication bus for transmitting sensor data and issuing control commands.

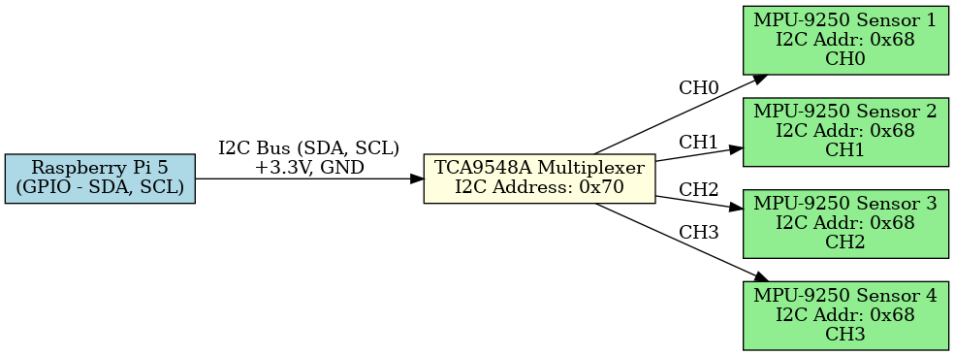

Figure 5: A detailed view of the I²C bus topology.

The TCA9548A functions as an I^2C channel selector, distributing the shared SDA and SCL lines from the Raspberry Pi to multiple independent downstream channels. In this configuration, four MPU-9250 triaxial accelerometers are connected to dedicated output channels (CH0–CH3) of the multiplexer. Each MPU-9250 sensor shares the same default I^2C address (0×68); therefore, direct parallel connection on a single I^2C bus would result in address conflicts. This limitation is effectively addressed by the TCA9548A's channel-switching capability, which allows only one sensor channel to be active on the bus at any given time.

The wiring configuration presented in Table 2 ensures reliable data transmission by maintaining a common ground reference and minimizing bus contention. This structured interconnection allows the Raspberry Pi to selectively enable individual multiplexer channels for sensor polling, thereby supporting synchronized multi-sensor data acquisition and scalable system expansion.

Table 2: GPIO wiring configuration between the Raspberry Pi 5, TCA9548A I^2C multiplexer, and MPU-9250 accelerometer modules.

Component	Function	Pin Position
Raspberry Pi 5 (GPIO 2)	SCL (I^2C Clock)	Pin 5
Raspberry Pi 5 (GPIO 3)	SDA (I^2C Data)	Pin 3
TCA 9548A SDA	Connects to Rpi SDA	SDA → Pin3
TCA 9548A SCL	Connects to Rpi SCL	SCL → Pin 5
MPU-9250 Sensor 1	Connected to TCA 9548A Channel 0	Via I^2C CH0 (MPU 9250 FL)
MPU-9250 Sensor 2	Connected to TCA 9548A Channel 1	Via I^2C CH1 (MPU 9250 FR)
MPU-9250 Sensor 3	Connected to TCA 9548A Channel 2	Via I^2C CH2 (MPU 9250 RL)
MPU-9250 Sensor 4	Connected to TCA 9548A Channel 3	Via I^2C CH4 (MPU 9250 RR)

Each sensor is powered through the regulated supply lines provided by the Raspberry Pi, while a common ground reference is maintained across all components to ensure signal integrity. The multiplexer is controlled programmatically by the Raspberry Pi, which sequentially enables individual channels to poll vibration data from each MPU-9250 sensor. This structured GPIO and I^2C wiring approach ensures robust communication, minimizes electrical interference, and facilitates straightforward system expansion for additional sensing nodes.

2.4 Data Collection Procedures

The experimental setup consists of mounting vibration sensors on tyres and capturing raw vibration signals under varying pressure conditions, as in [2,6]. Controlled driving tests are conducted under defined velocity and load conditions to reflect in-field scenarios. All sensors were evaluated during real driving scenarios, including steady-speed operation at approximately 60 km/h, which represents common urban driving conditions. This ensures that the collected data reflect realistic operational dynamics rather than laboratory-induced vibration profiles.

The tire pressure settings employed in this study are summarized in Figure 6, which outlines the 20 experimental test conditions used during vibration data acquisition. Each test condition represents a distinct tire pressure configuration applied to the vehicle during real-world operation. These configurations were systematically varied to capture a broad range of operating states, including nominal and reduced tire pressure scenarios, while maintaining consistent driving conditions. By conducting multiple tests across a defined range of pressure levels, the study captures variations in tire stiffness and contact dynamics that influence vibration transmission through the suspension system and vehicle chassis. The resulting vibration data provide a comprehensive dataset for subsequent time-domain, frequency-domain, and statistical analyses.

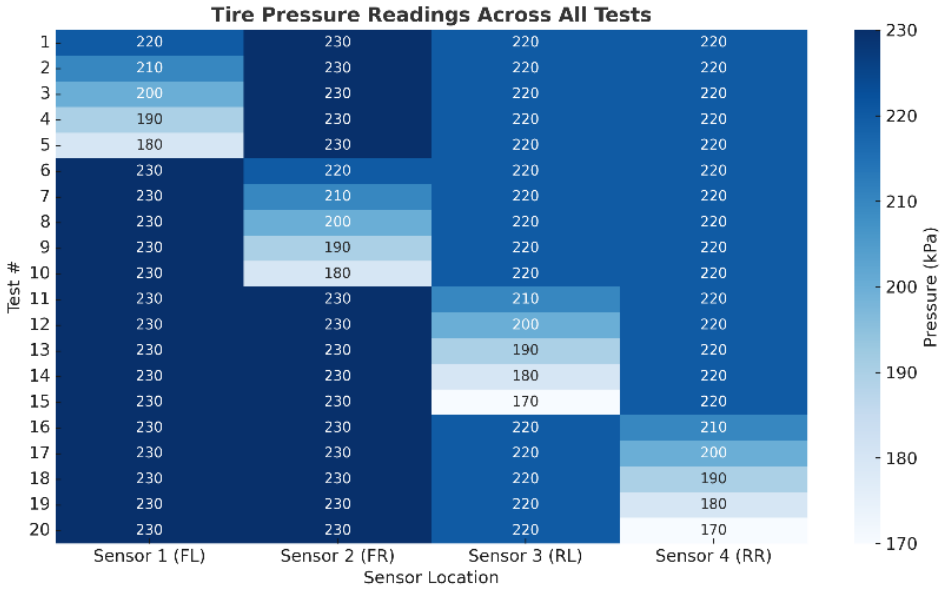

Figure 6: Tire pressure configurations for the 20 experimental test conditions used in vibration data acquisition.

Presenting the experimental pressure settings in a tabulated form enables consistent cross-comparison between test conditions and facilitates traceability between the applied pressure values and the corresponding vibration signatures. This structured approach supports rigorous evaluation of the relationship between tire pressure variation and vibration behavior under real driving conditions.

2.5 Data Acquisition, Processing, Visualization, and Remote Monitoring Pipeline

The proposed system employs an end-to-end data acquisition and processing pipeline that integrates real-time sensing, storage, visualization, and secure remote accessibility. The overall flow is illustrated in Figure 7, which depicts the transition from initial sensor activation to web-based visualization and remote monitoring.

Vibration signals were acquired from the triaxial accelerometers at a sampling rate of 10 Hz, corresponding to a sampling interval of 0.1 s, which is sufficient to capture low-frequency structural vibrations associated with tyre–road interaction during steady-speed driving. Time-domain analysis was performed on fixed-length windows of N = 64 samples, corresponding to a window duration of T = 6.4 s, to ensure consistent feature extraction across all tyre pressure classes. Frequency-domain representations were obtained using the Fast Fourier Transform (FFT) applied to each windowed segment. Acceleration amplitudes are expressed in m/s^2, ensuring physical interpretability and consistency across both time- and frequency-domain analyses. For clarity and consistency, all acceleration data are converted to SI units (m/s^2) for offline analysis and reporting in this paper. However, raw sensor outputs may be visualized in gravitational units (g) in the real-time dashboard interface.

Sensor data are continuously captured from the MPU-9250 accelerometers using Python-based acquisition scripts running on a Raspberry Pi 5. The acquisition routine samples vibration signals at approximately 10 Hz (100 ms interval), providing sufficient temporal resolution to characterize tire-induced vibration patterns [19]. Each captured reading is buffered and visualized in real time while simultaneously being stored in a MariaDB database. Every record is appended with a precise timestamp to ensure temporal synchronization and reproducibility during subsequent analyses [20].

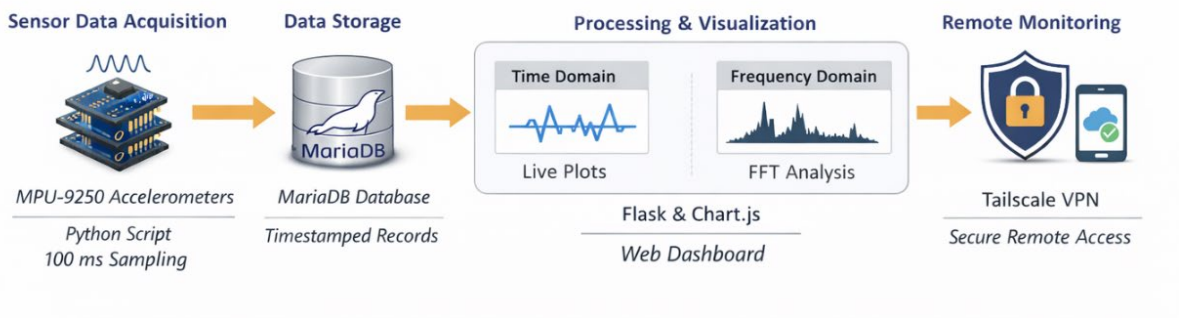

Figure 7: Data acquisition, processing, visualization, and remote monitoring pipeline for the IoT-based vibration monitoring system.

Stored signals are evaluated in both the time domain and frequency domain, providing complementary diagnostic perspectives. In the time domain, raw tri-axial acceleration waveforms are inspected to observe transient oscillations, amplitude variations, and abnormal fluctuations. In the frequency domain, a Fast Fourier Transform (FFT) is applied to extract dominant spectral components associated with tire–road dynamics and under-inflation behavior [21]. Visualization is implemented through a browser-based dashboard developed using Flask, Chart.js, and Flask-SocketIO, enabling interactive, low-latency visualization of live and archived vibration records.

To support secure, scalable access, Tailscale VPN is deployed on a Raspberry Pi 5, enabling encrypted peer-to-peer connectivity without exposing the system to public networks. This approach enhances cybersecurity and reliability while allowing authorized users to access dashboards and system controls from remote locations, mobile devices, or laboratory workstations [18]. As a result, the system supports continuous, distributed vibration monitoring suitable for real-world automotive environments.

In summary, the architecture presented in Figure 8 demonstrates a fully integrated IoT-based vibration monitoring framework, in which sensing, acquisition, processing, storage, visualization, and secure remote access operate cohesively within a single platform. The coordinated use of MPU-9250 accelerometers, the TCA9548A I^2C multiplexer, and the Raspberry Pi 5 enables

scalable multi-sensor data acquisition, while Python-based scripts ensure deterministic handling of vibration signals prior to structured storage in MariaDB. The incorporation of a Flask web interface provides accessible real-time visualization, and the integration of Tailscale VPN ensures secure remote connectivity without compromising system reliability. Collectively, this architecture establishes a robust methodological foundation for subsequent signal analysis, decision-support algorithms, and real-world deployment in automotive vibration monitoring environments.

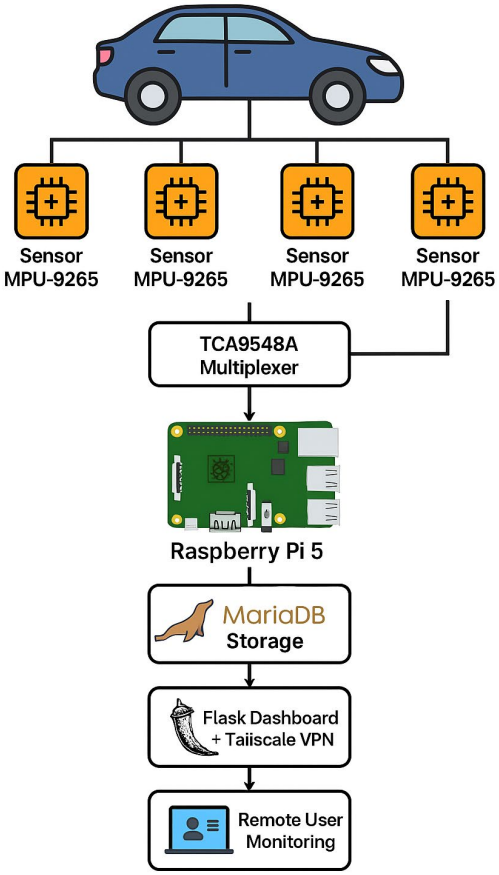

Figure 8: Overall architecture of the IoT-based vibration monitoring system.

3. RESULTS AND DISCUSSION

The proposed IoT-based vibration monitoring system successfully recorded tri-axial accelerometer signals from four MPU-9250 sensors positioned at the front-left, front-right, rear-left, and rear-right locations of the vehicle. All vibration measurements were continuously time-stamped and stored in the MariaDB database, enabling reliable retrieval and longitudinal comparison across multiple driving and tire pressure conditions. This centralized database structure ensured data integrity and facilitated systematic signal analysis in subsequent stages.

Table 3 summarizes the recorded tire pressure values from 20 experimental runs involving 4 wheels. The objective of this table is to provide an overview of how tire inflation levels varied across trials and how they were categorized into operational conditions. The thresholds were organized into categorical classes, with Class 0 representing ideal pressure and Classes 1–8 progressively lower pressure levels. The structured classification enables clearer interpretation of tire-pressure behavior across wheels, particularly when associating pressure reductions with changes in vibration response.

In the dataset, most cases fall into the under-inflated category, particularly involving Sensors 3 and 4. This trend indicates that reduced tire pressure results in an asymmetric pressure distribution across wheels, supporting existing evidence that tire under-inflation alters tire–road contact and vibration signatures. Moreover, the dataset demonstrates consistently recorded values, suggesting sensor stability and repeatable measurements across trials. This reliability is critical when integrating vibration signatures with automated decision-making systems.

To evaluate whether the extracted features are suitable for automatic tire pressure diagnosis, a decision tree classifier was trained using the normalized vibration data and corresponding pressure classes (0–8). The model achieved an overall accuracy of 93.7%, indicating strong discriminative capability. Decision trees are particularly attractive for embedded applications because they are computationally efficient and yield interpretable rule-based structures [22]. The high accuracy demonstrates that the combination of time-domain, frequency-domain, and statistical features provides a robust basis for distinguishing between ideal and under-inflated tire conditions.

Table 3: Distribution of Tire Pressure Values Across Tests.

Class	Sensor 1 (kPa)	Sensor 2 (kPa)	Sensor 3 (kPa)	Sensor 4 (kPa)	Category (Pressure)
0	230	230	220	220	Ideal
1	220	230	220	220	Under-inflated
1	210	230	220	220	Under-inflated
1	200	230	220	220	Under-inflated
2	190	230	220	220	Under-inflated
2	180	230	220	220	Under-inflated
3	230	220	220	220	Under-inflated
3	230	210	220	220	Under-inflated
3	230	200	220	220	Under-inflated
4	230	190	220	220	Under-inflated
4	230	180	220	220	Under-inflated
5	230	230	210	220	Under-inflated
5	230	230	200	220	Under-inflated
6	230	230	190	220	Under-inflated
6	230	230	180	220	Under-inflated
6	230	230	170	220	Under-inflated
7	230	230	220	210	Under-inflated
7	230	230	220	200	Under-inflated
8	230	230	220	190	Under-inflated
8	230	230	220	180	Under-inflated
8	230	230	220	170	Under-inflated

Representative time-domain waveforms provide an intuitive view of how tire pressure affects vibration response. Figure 9 illustrates the X-axis acceleration at the front-left sensor (S1X-fl) for a subset of samples. Under near-ideal pressure (Class 0), the signal exhibits relatively low amplitude and more regular oscillations. As pressure decreases, the peak-to-peak values increase and the waveform becomes more irregular, indicating stronger and less stable tire–road interaction. These observations are consistent with prior vibration-based studies, which report that under-inflated tires induce larger structural deformation and enhanced vibration transmission [23].

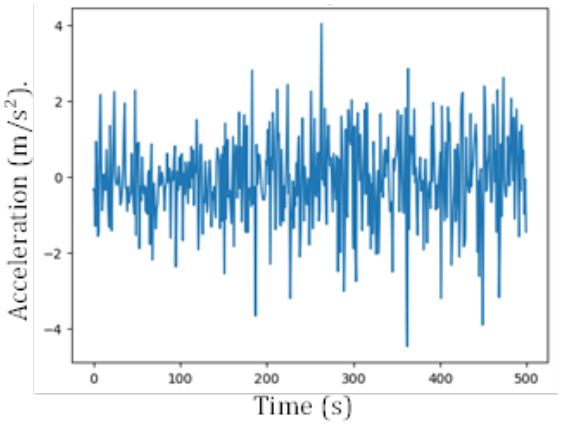

Figure 9: Time-domain vibration signal for S1X-fl under representative tire pressure conditions.

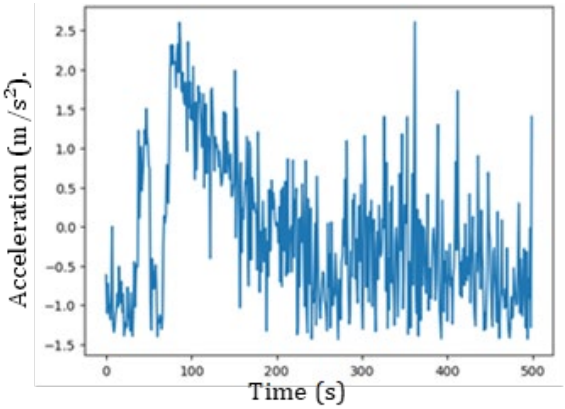

Figure 10: Time-domain vibration signal for S1Y-fl under representative tire pressure conditions.

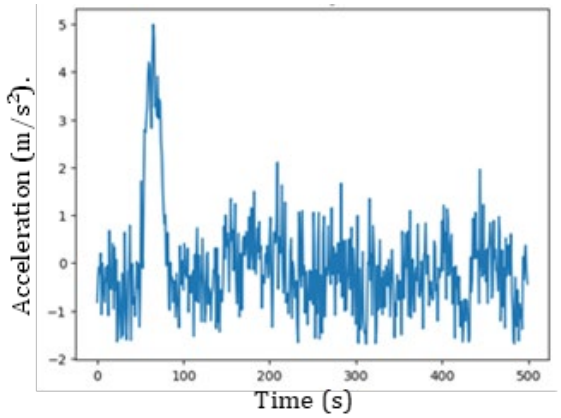

Figure 11: Time-domain vibration signal for S1Z-fl under representative tire pressure conditions.

The increased amplitude and variability observed in the time-domain plots for under-inflated conditions support the hypothesis that vibration signatures can be used as indicators of tire pressure state. Such behaviour aligns with findings in vibration-based tire diagnostics, where amplitude growth and transient spikes reflect degraded tire stiffness and contact dynamics [23].

To further characterize the vibration behaviour, the recorded signals were transformed into the frequency domain using the Fast Fourier Transform (FFT). Figure 12 shows example spectra of the front-left sensor axes (S1X-fl, S1Y-fl, S1Z-fl). Under ideal pressure, spectral energy is primarily concentrated at lower frequencies, corresponding to stable rotational and suspension dynamics. As tire pressure decreases, additional peaks emerge and the energy distribution broadens,

indicating the presence of more complex, unstable vibration modes. These spectral changes are consistent with observations in vibration-based condition monitoring, where faults or abnormal operating states introduce new frequency components [24].

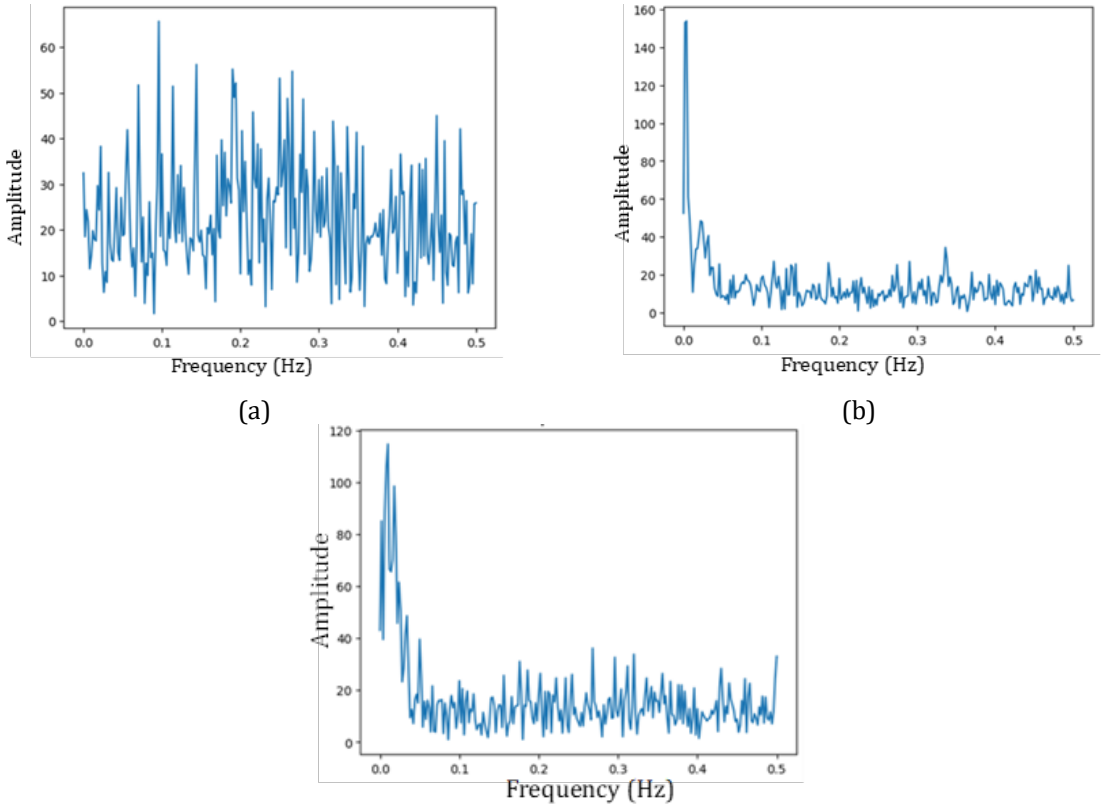

Figure 12: Frequency-domain FFT spectrum for highlighting spectral changes under different tire pressure states. (a) S1X-fl, (b) S1Y-fl and (c) S1Z-fl.

The emergence of additional spectral peaks and broader frequency content in under-inflated cases reinforces the time-domain findings and suggests that frequency-domain features are useful for automated classification. By capturing how energy shifts across the spectrum, FFT-derived features complement raw waveform analysis and provide a richer representation of tire–road dynamics.

In addition to time- and frequency-domain analysis, statistical descriptors were computed for each sensor axis across classes. Mean and standard deviation values were used to quantify central tendency and variability. Figure 13 summarises these statistics for a representative axis. In general, under-inflated conditions exhibit higher mean amplitudes and larger standard deviations, confirming that lower tire pressure results in more intense, less stable vibration behaviour [23]. These statistical trends support the visual observations from the time-domain and FFT plots and demonstrate that simple scalar features can capture much of the discriminative information needed to separate pressure states.

One of the key outcomes of this research was the successful implementation of a fully functional IoT-based vibration-monitoring dashboard, deployed with Flask on a Raspberry Pi 5. The interface allows real-time visualization of three-axis accelerometer data (X, Y, and Z) from all four MPU-9250 sensors simultaneously. Figure 14 shows the web dashboard displaying continuous vibration streams acquired during tyre pressure testing. The dashboard presents two complementary visualization modes:

a) Time-domain monitoring: real-time acceleration waveforms reveal transient responses and variations in vibration amplitude under different pressure states, as shown in Figure 15.
b) Frequency-domain monitoring (FFT): dominant frequency peaks are extracted, allowing users to detect resonance or abnormal vibration signatures associated with structural or inflation anomalies, as shown in Figure 16.

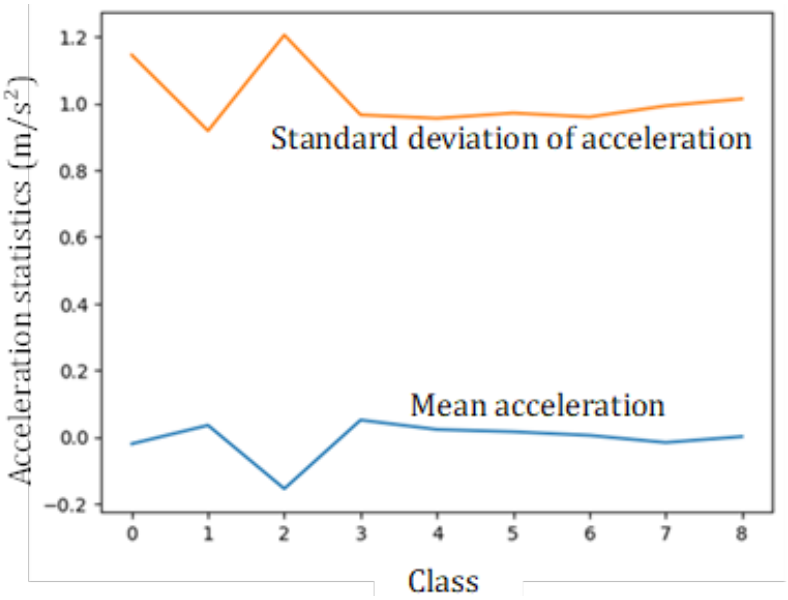

Figure 13: Statistical summary (mean and standard deviation) of a representative vibration axis across tire pressure classes.

Figure 14: Real-time vibration visualization dashboard implemented using Flask, showing time-domain accelerometer plots for four sensors.

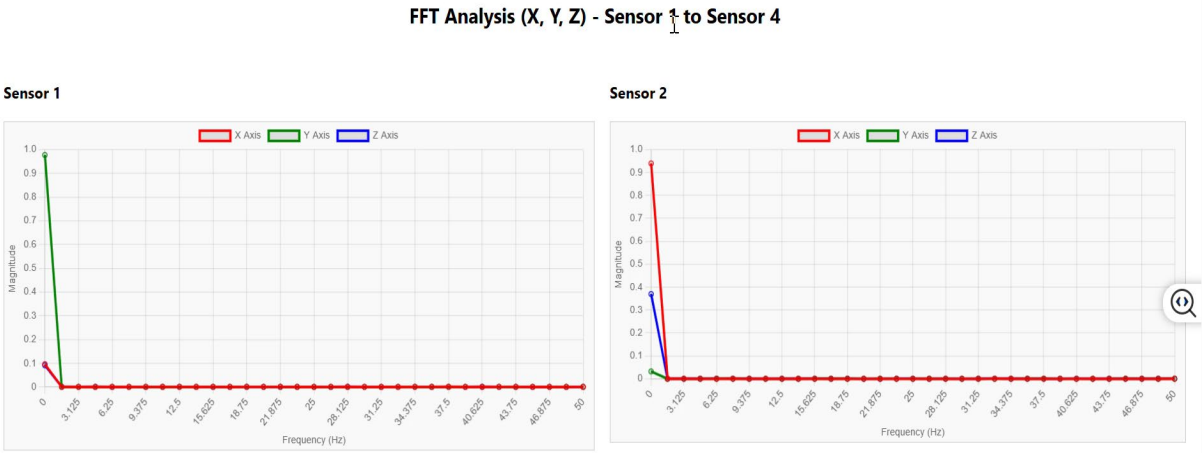

Figure 15: Frequency-domain FFT dashboard illustrating dominant vibration frequency peaks across tyre sensors.

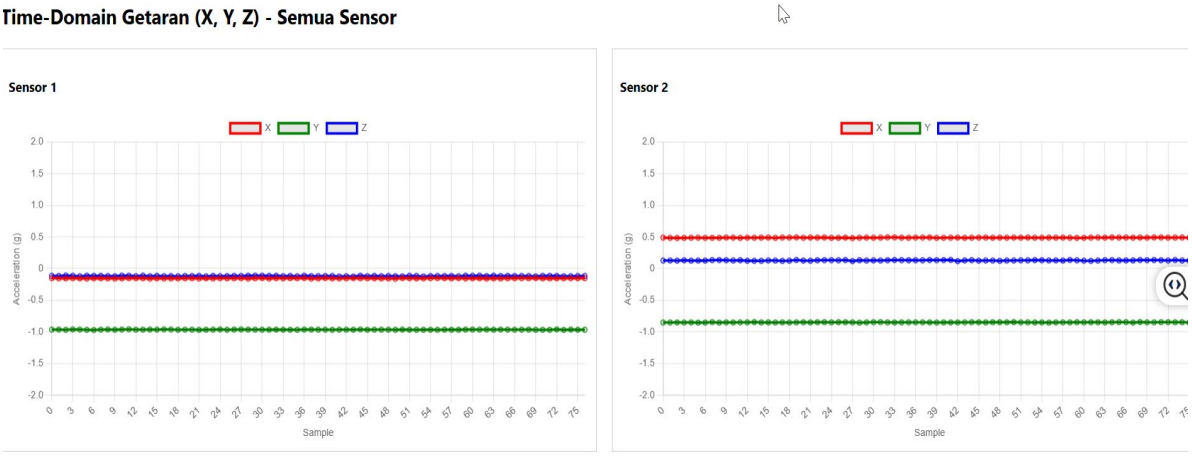

Figure 16: Time-domain dashboard illustrating dominant vibration frequency peaks across tyre sensors.

These visualizations enable the operator to continuously observe tyre behavior without physically connecting instruments to the vehicle. Instead, vibration data is streamed over the network, processed on the Raspberry Pi, and delivered via a browser interface. This aligns with modern IoT diagnostic architectures reported in recent literature, which emphasize distributed sensing, edge processing, and cloud-enabled analytics for automotive health monitoring [25,26]. From a broader perspective, the ability to integrate sensor acquisition, signal processing, and visualization into a unified IoT ecosystem represents a significant advancement over traditional wired measurement setups. This approach aligns with emerging research trends advocating embedded and connected monitoring systems for vehicles [27].

Vibration signatures captured by four MPU-9250 accelerometers positioned at the front-left, front-right, rear-left, and rear-right tyre regions were successfully recorded, transmitted, visualized, and interpreted under multiple tyre pressure conditions. Time-domain analyses revealed clearly distinguishable vibration trends between the ideal pressure condition (Class 0) and various under-inflated states (Classes 1–8). Stable, low-amplitude responses were observed at normal pressure, whereas increasing pressure deviations led to larger, more unstable oscillation patterns, indicating heightened tyre–road interaction. Complementary frequency-domain (FFT) results further highlighted shifts in dominant spectral components, confirming that tyre pressure variation alters the dynamic response characteristics of the vehicle structure.

The statistical summaries across sensors and axes provided additional evidence that mean amplitude and variance increase progressively under under-inflated states, reinforcing previous

findings in vibration-based diagnostics. These signal features were subsequently used to support automated classification. The decision tree algorithm achieved an accuracy of **93.7%**, demonstrating strong discriminative capability and confirming the suitability of vibration signatures for tyre pressure assessment. This section also validated the robustness of the IoT architecture. Real-time data acquisition through Raspberry Pi, transmission to MariaDB, visualization via Flask dashboards, and secure remote access through Tailscale collectively enabled continuous monitoring without physical inspection. This web-based capability proves essential for remote diagnostics, preventive maintenance, and future smart-vehicle applications.

4. CONCLUSION

The findings from this study demonstrate that IoT-based vibration monitoring, when combined with structured analytical methods, provides a feasible and effective approach for multi-class tyre pressure diagnostics. The developed system successfully integrates multiple triaxial accelerometers, a TCA9548A I^2C multiplexer, and a Raspberry Pi 5 into a unified sensing infrastructure capable of capturing vibration signatures that reflect dynamic tyre behaviour under different pressure states. The IoT architecture further supports secure, continuous, and remotely accessible data acquisition, establishing a robust framework for real-time monitoring in practical driving environments.

Signal analysis in both the time and frequency domains revealed clear distinctions between ideal and under-inflated tyres. Stable, low-amplitude vibration responses were observed under nominal pressure, whereas progressively under-inflated conditions resulted in increased amplitude variability and broader spectral content. These findings confirm that vibration signatures contain meaningful information related to tyre stiffness variation and tyre–road interaction dynamics. Building on these extracted features, the decision-tree classifier achieved high classification accuracy while remaining computationally efficient and interpretable, making it well-suited for real-time, embedded diagnostic applications.

Notwithstanding these results, several system-level limitations should be acknowledged. The vibration measurements rely on cabin-mounted accelerometers, which capture tyre–road interaction indirectly through the vehicle structure; as a result, sensor placement constraints may attenuate or distort certain vibration components compared to direct tyre-mounted sensing. In addition, diagnostic performance is influenced by driving conditions such as road surface characteristics and vehicle speed, as variations in pavement roughness and operating velocity can alter vibration signatures. The experimental validation was conducted on a single passenger vehicle platform under steady-speed driving conditions; therefore, the transferability of the trained model to other vehicle types, suspension configurations, and tyre specifications may require recalibration or retraining. Furthermore, environmental noise sources, including engine-induced vibrations and external disturbances, can affect signal quality under certain operating conditions.

Overall, the study highlights that IoT-driven vibration sensing supported by interpretable decision-tree analytics represents a promising pathway toward intelligent, real-time tyre pressure assessment. By enabling early detection of abnormal tyre conditions, the proposed system contributes to safer vehicle operation and demonstrates strong potential for integration into broader smart-vehicle ecosystems. Future work will focus on expanding the dataset across diverse road surfaces and speed profiles, validating performance across multiple vehicle platforms, and enhancing robustness through adaptive signal processing and multi-condition model training.

ACKNOWLEDGEMENTS

This paper was created within the TVET Fellowship Program 2025 under the Center for Instructor and Advanced Skill Training, Ministry of Human Resources.

REFERENCES

[1] Yu, S., Niu, L., Chen, J. Experimental and numerical studies on bond quality of fully grouted rockbolt under confining pressure and pull-out load. Shock and Vibration (2022) pp.1–12.
[2] Hussain, M., Lee, Y., Kim, D. Frequency-domain analysis of tire–road interaction for tire condition monitoring. Mechanical Systems and Signal Processing, vol 135 (2020) pp.14-18.
[3] Jiang, H., Ji, X., Yang, Y., Qu, Y., Wu, M. Vibration signal analysis of roadheader based on referential manifold learning. Shock and Vibration (2023) pp.1–11.
[4] Zhou, L., Sun, D., Liu, Q. Edge computing for smart vehicle diagnostics: A vibration monitoring perspective. Mechanical Systems and Signal Processing, vol 190 (2023) pp.1-15.
[5] Hassan, I. U., Panduru, K., Walsh, J. An in-depth study of vibration sensors for condition monitoring. Sensors, vol 24 (2024) pp.740-755.
[6] Hajnayeb, A. Cavitation analysis in centrifugal pumps based on vibration bispectrum and transfer learning. Shock and Vibration (2021) pp.1–8.
[7] Sun, G., Hu, Y., Wu, B., Zhou, H. Parallel-machine scheduling with DeJong's learning effect, delivery times, rate-modifying activity, and resource allocation. Shock and Vibration (2021) pp.1–13.
[8] Sun, L., Wu, B., Ning, L. Identification of vibration signal for residual pressure utilization hydraulic unit using MRFO-BP neural network. Shock and Vibration (2022) pp.1–36.
[9] Dong, Z., Liu, Y., Kang, J., Zhang, S. A stochastic learning algorithm for machine fault diagnosis. Shock and Vibration (2022) pp.1–9.
[10] Huang, T., Xu, B., Wang, Y., Zhu, J., Wan, Z. Mine microseismic signal denoising based on a deep convolutional autoencoder. Shock and Vibration (2023) pp.1–15.
[11] Kibrete, F., Woldemichael, D. E., Gebremedhen, H. S. Optimization of sample size, data points, and data augmentation stride in vibration signal analysis for deep learning-based fault diagnosis of rotating machines. Shock and Vibration (2025) pp.1–16.
[12] Zhu, H., Miao, C. Seismic fragility analysis of the reinforced concrete continuous bridge piers based on machine learning and symbolic regression fusion algorithms. Shock and Vibration (2021) pp.1-8.
[13] Feng, X., Chen, Z., Li, Z., Zeng, Q., Wang, J., Wang, P. Machine learning–enhanced microseismic analysis for evaluating rock crack trajectory. Shock and Vibration (2024) pp.1-11.
[14] Tu, W., Chen, Y. Vibration transmission characteristics and measuring points analysis of bearing housing system. Shock and Vibration (2022) pp.1–12.
[15] Han, G., Xu, L. Effects of resonator shape on nonlinear resonant frequencies of a microresonant pressure sensor. Shock and Vibration (2022) pp.1–18.
[16] Huang, W., Yan, X., Zhang, S., Li, Z., Hassan, J. N. A., Chen, D., Wen, G., Chen, K., Deng, G., Huang, Y. Mems and moems gyroscopes: A review. Photonic Sensors, vol 13 (2023) pp.1-26.
[17] Wang, C., Tu, X., Chen, Q., Yang, Q., Fang, T. Movable surface rotation angle measurement system using imu. Sensors, vol 22, issue 22 (2022) pp.123-130.
[18] Fang, Y., Xu, Y., Wang, J. Vehicle vibration-based condition monitoring using low-cost MEMS sensors. Sensors, vol 20, issue 6 (2020) pp.1-17.
[19] Al-Fuqaha, A., Guizani, M., Mohammadi, M., Aledhari, M., Ayyash, M. Internet of things: A survey on enabling technologies, protocols, and applications. IEEE Communications Surveys & Tutorials, vol 17, issue 4 (2015) pp.2347–2376.
[20] Sicari, S., Rizzardi, A., Grieco, L. A., Coen-Porisini, A. Security, privacy and trust in internet of things: The road ahead. Computer Networks, vol 76 (2015) pp.146–164.

[21] Chang, H., Park, J., Kim, S. Vibration-based tire pressure monitoring using accelerometers. Sensors, vol 18, issue 10 (2018) pp.1-15.
[22] Lee, Y., Kim, D. Tire pressure monitoring through vibration signature analysis. Vehicle System Dynamics, vol 57, issue 8 (2019) pp.1153–1173.
[23] Anoop, P. S., Sugumaran, V. Classifying machine learning features extracted from vibration signal to monitor automobile tyre pressure. Structural Durability & Health Monitoring, vol 11, issue 2 (2017) pp.191–208.
[24] Kolok, P. Low-cost IoT-based predictive maintenance using vibration monitoring. Sensors, vol 25, issue 21 (2025) pp.1-26.
[25] Li, H., Zhang, Y., Wang, X. Internet-of-things enabled vehicle condition monitoring: Architecture, sensing strategies, and applications. IEEE Internet of Things Journal, vol 9, issue 15 (2022) pp.13412–13425.
[26] Khan, S., Ali, M., Rehman, A. Smart automotive health monitoring using embedded iot platforms. Sensors, vol 21, issue 4 (2021) pp.1-18.
[27] Zhang, T., Chen, Y. Cloud-connected vibration analytics for predictive maintenance in automotive systems. Journal of Intelligent Manufacturing, vol 35, issue 2 (2024) pp.455–470.

Conflict of interest statement: The authors declare no conflict of interest.

Author contributions statement: Conceptualization and Methodology, Mohd Saifunnaim bin Mat Zain and Ahmad Kadri bin Junoh; Formal Analysis, Mohd Saifunnaim bin Mat Zain; Investigation, Mohd Saifunnaim bin Mat Zain; Writing – Original Draft Preparation, Mohd Saifunnaim bin Mat Zain; Writing & Editing, Mohd Saifunnaim bin Mat Zain; Supervision, Ahmad Kadri bin Junoh.